The influence of interfaces on magnetic thin films and multilayers

1992 J. Phys.: Condens. Matter 4 7985

(http://iopscience.iop.org/0953-8984/4/40/011)

J. Phys.: Condens. Matter 4 (1992) 7985–7996. Printed in the UK

The influence of interfaces on magnetic thin films and multilayers

Qibiao Chen†||, M Onellion†, A Wall‡ and P A Dowben§

† Department of Physics, University of Wisconsin, Madison, WI 53706, USA
‡ IBM Corporation, Storage Systems Products Division, Rochester, MN 55901, USA
§ Department of Physics, Syracuse University, Syracuse, NY 13244-1130, USA

Received 7 July 1992

Abstract. One to nine monolayer Co films on Cu(100) and one- to five-layer-thick Co/Cu/Co trilayers on Cu(100) were fabricated at room temperature using metal vapour-phase expitaxy techniques under ultrahigh-vacuum conditions. Using electron diffraction and Auger electron spectroscopy, we determined that the single layers and multilayer films grow epitaxially and predominantly in a layer-by-layer growth mode. Longitudinal and polar magneto-optic Kerr effect (MOKE) measurements established that the easy axis of magnetization is in the substrate plane and provided the change of total magnetization with layer and multilayer thickness. Our data suggest that the interface magnetization is affected by the thickness of the top Co layer.

1. Introduction

In the past few years, there has been increasing interest in the studies of magnetic coupling in magnetic multilayer systems [1]. This has been due both to the scientific interest and importance in industrial application, such as information storage media [2–4]. Some multilayer systems studied exhibit an oscillatory magnetic coupling when the non-magnetic interlayer thickness changes [5–8]. Such behaviour has appeared for systems such as magnetic-rare-earth–non-magnetic-rare-earth and 3d-transition metal–noble-metal [5, 8] multilayers. The common picture in describing the multilayer magnetic systems is that there are sheets of aligned magnetic moments (the magnetic layer) and polarizable layers of free electron gas (the non-magnetic layer). A variant of the RKKY interaction appears applicable in explaining the magnetic coupling between the ferromagnetic layers separated by the non-magnetic layers [9]. So far, all the experimental reports have adopted this picture in explaining their results even though serious problems exist. One problem concerning the coupling between magnetic layers is how the interface magnetization affects the magnetic coupling. There are several theoretical reports concerning the effects of boundary conditions on magnetic multilayers systems [10, 11]. This issue is ignored completely in the traditional RKKY theory.

In this report, we present in the experimental results section a thorough study of both single epitaxial films of Co and epitaxial Co/Cu/Co trilayers on Cu(100). There

|| Present address: Department of Electrical Engineering, Carnegie Mellon University, Pittsburgh, PA, USA.

0953-8984/92/407985+12$04.50

are three pertinent points that emerge from the data. The total magnetic moment of the single Co films does not increase in a linear or logarithmic form with film thickness between one to nine layers. This indicates that the magnetic moments of Co layers deviate significantly from large, localized magnetic moments of the heavy rare-earth metals, as discussed below. The total magnetic moment of the Co/Cu/Co trilayers on Cu(100) exhibits an oscillatory behaviour that depends on both the thickness of the Cu interlayer and that of the top Co layer. In addition, the hysteresis loops of all the Co/Cu/Co trilayers on Cu(100) exhibit a square shape with a signal at remanence that is virtually the same magnitude as that at the largest applied magnetic field.

2. Experimental details

The vacuum chamber used in this experiment has been described elsewhere [12]. The base pressure for our ultrahigh-vacuum (UHV) chamber is 5×10^{-11} Torr. The single-crystal Cu(100) sample used in this experiment was cleaned via repeated cycles of 400 eV argon-ion sputtering at room temperature to clean the surface and annealing to 700 °C. This process was repeated until a sharp 1×1 low-energy electron diffraction (LEED) pattern with spot size less than 1 mm was obtained. In addition, reflection high-energy electron diffraction (RHEED) and Auger electron spectroscopy (AES) were used to characterize the sample. The AES measurements indicated that the carbon and oxygen contaminants on Cu(100) substrate were less than 1 at.% (which was the limit of the sensitivity of our AES system) throughout the experiment.

Before deposition of Co and Cu, both evaporators were outgassed for 24 hours at a temperature slightly below the evaporation temperature. The chamber pressure was 5×10^{-11} Torr before deposition and never exceeded 2×10^{-10} Torr during the deposition of Co and Cu. After the deposition, longitudinal and polar magneto-optic Kerr effect measurements were performed on these systems to measure the Kerr angle and MOKE hysteresis loops. In order to confirm that the films we measured were clean and ordered, we conducted AES and LEED measurements after the MOKE measurements. The experimental results indicated that the films we measured exhibited very good crystalline order without observable reconstruction and free of contaminants. AES measurements were also performed to calibrate the film thickness. The stated film thicknesses were reproducible to within 10% relative accuracy in thickness. Our experimental results for segregation at the interface between Co and Cu layers [12] indicated that the interface between Co and Cu was atomically sharp without interdiffusion for the films grown at room temperature.

Our MOKE apparatus uses a magnet in a vacuum that can be rotated so that both polar and longitudinal MOKE measurements can be performed *in situ* on the same sample. The gap between the two magnetic poles is half an inch wide. The applied magnetic field in the centre of the magnet gap was as large as 1500 Oe, with no rise in the vacuum pressure, and the applied magnetic field is quite uniform across the sample area.

To measure the longitudinal Kerr rotation angle at remanence, we followed a standard procedure. We used s-polarized light from a He–Ne laser and the extinction ratio obtained was 1×10^{-7}. We first applied a large magnetic field of 1500 Oe in one direction. We then reduced the magnetic field to zero and the magnetic system was in the remanence state. We rotated the second polarizer to reach extinction. After reaching extinction, we reversed the magnetic field and applied a 1500 Oe magnetic

field in the opposite direction to switch the magnetization direction in the sample plane. We then reduced the magnetic field to zero to measure the photodiode current, I_0. We rotated the second polarizer to a fixed known angle, 10°, and measured the corresponding photodiode current, I_{10}. The Kerr rotation angle θ at remanence was calculated using the formula:

$$\theta = [(I_0 - I_r)/(I_{10} - I_r)]^{1/2} \sin 10^\circ \tag{1}$$

where I_r is the photodiode current at extinction. We performed the measurement of I_{10} for each measurement of Kerr rotation angle to avoid systematic errors. The accuracy of the measured Kerr rotation angles was limited by the sensitivity of the photodiode and the uncertainty of measured Kerr rotation angles was 0.03 mrad.

3. Experimental results

Figure 1 illustrates the measured Kerr rotation angles at remanence (crosses) for one to nine layers of Co on Cu(100) thin films grown epitaxially at room temperature and the theoretical fit (full line) using a simple Ginzburg–Landau (GL) model. Since the photon penetration depth, about 20 nm, is much larger than the film thickness (< 4 nm), the light used in the MOKE measurements samples the entire film without attenuation. Taking the uncertainty of Kerr rotation angle measurement into account, the measured Kerr rotation angles increase with the film thickness in a way that is clearly different from either a linear or a logarithmic functional form. Diffraction studies were performed on these thin Co films on Cu(100), no crystallographic changes with film thickness were observed, consistent with other investigators' results [13]. Our segregation studies, and the RHEED oscillation measurements, transmission electron microscopy (TEM), and x-ray diffraction studies by other investigators [14] indicate that Co grows epitaxially on Cu(100) without interdiffusion at temperature up to 250 °C and that the interface between Co and Cu is atomically abrupt.

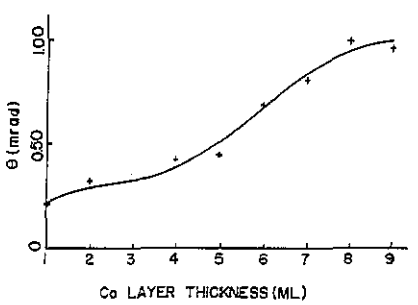

Figure 1. The longitudinal Kerr rotation angle versus Co-layer thickness for one to nine layers Co on Cu(100) thin-film systems. The crosses are the experimental data and the full line is the theoretical fit.

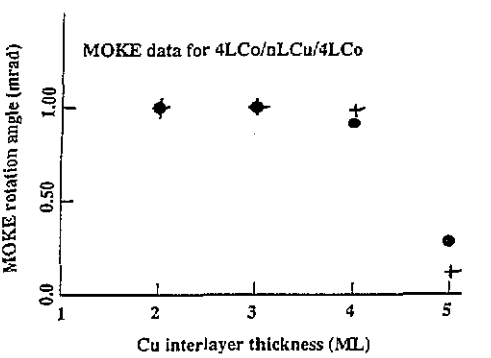

Figure 2. The longitudinal Kerr rotation angle versus Cu interlayer thickness for Co/Cu/Co trilayers on Cu(100). The top- and bottom-Co-layer thicknesses are fixed as four layers thick. The interlayer Cu thickness changes from two to five. The full dots are the experimental data.

Figure 2 illustrates the measured Kerr rotation angle (full dots) as a function of Cu layer thickness for Co/Cu/Co trilayers on Cu(100) and the theoretical fit (crosses) of these data from our GL mean-field theory analysis. The thickness of the top and bottom Co layers were fixed at four layers, and the thickness of the interlayer Cu changed from two to five layers. The Kerr rotation angle remained at 1.00 mrad for Cu films of two and three layers thick, and decreased to 0.90 mrad for Cu film of four layers thick. As the thickness of interlayer Cu increased to five layers, the measured Kerr rotation angle decreased to 0.20 mrad, indicating that close to perfect cancellation of the magnetic moments between the top and bottom Co layers occurred. This indicates that the effective magnetic coupling between the top and bottom Co layers has switched from ferromagnetic to antiferromagnetic coupling as the thickness of interlayer Cu changed from four to five atomic layers.

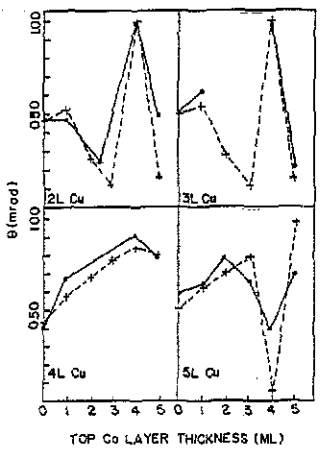

Figure 3. The longitudinal Kerr rotation angle versus top-Co-layer thickness for Co/Cu/Co trilayer on Cu(100). The interlayer Cu layer thicknesses are fixed as two, three, four, and five atomic layers. The full lines and dots are experimental results. The dotted lines and crosses are the best fit from a GL analysis.

To obtain information about the effect of the Co film on the overall magnetic coupling, we performed other experiments in which we fixed the thickness of the interlayer Cu and varied the thickness of the top Co layer. Figure 3 illustrates the measured Kerr rotation angles as a function of the thickness of the top Co layer for the Co/Cu/Co trilayers on Cu(100), for interlayer Cu of (A) two layers of Cu, (B) three layers of Cu, (C) four layers of Cu, and (D) five layers thick. The thickness of the bottom Co layer in figure 3 was always four layers. It is noteworthy that the measured Kerr rotation angles oscillated from maximum to minimum as the thickness of the top Co film changed, which has not been reported before. In figure 3, top left, the measured Kerr rotation angles changed from a minimum of 0.30 mrad to a maximum of 1.00 mrad as the thickness of the top Co film increased from two to four atomic layers. The change of the measured Kerr rotation angles was well beyond the total experimental uncertainty, 0.03 mrad. In figure 3, top right, the measured Kerr rotation angles changed from a maximum of 1.00 mrad to a minimum of 0.25 mrad as the thickness of the top Co film incresed from four to five atomic layers. The data illustrated in figure 3, bottom left, exhibit less dramatic changes with the thickness of the top Co layer. This is in accord with the theoretical predictions of the GL equations as discussed below. The data in figure 3, bottom right, also exhibit oscillations of the Kerr rotational angle as the thickness of the top Co layer was changed.

Figure 4 illustrates the longitudinal MOKE hysteresis loops for one to four layers of Co films on Cu(100), including (A) one monolayer of Co, (B) two monolayers of Co, (C) three monolayers of Co, and (D) four monolayers of Co. The hysteresis loops exhibit excellent squareness with very low coercivity. This strongly supports our assertion that the thin films we fabricated were of high quality. The magnetization direction was along the magnetization easy axis and the magnetization reversal was via domain wall movement [15]. The smoothness of the magnetization reversal via domain wall movement argues against the possibility that the films we fabricated possessed considerable defect density or interdiffusion. The inset of figure 4 indicates that the coercivity remains almost constant as the film thickness increases. This is consistent with other investigators' experimental results, that high-quality crystalline thin films possess single domains [14]. The magnetic anisotropy constant remains very small for these films as indicated by the low coercivity.

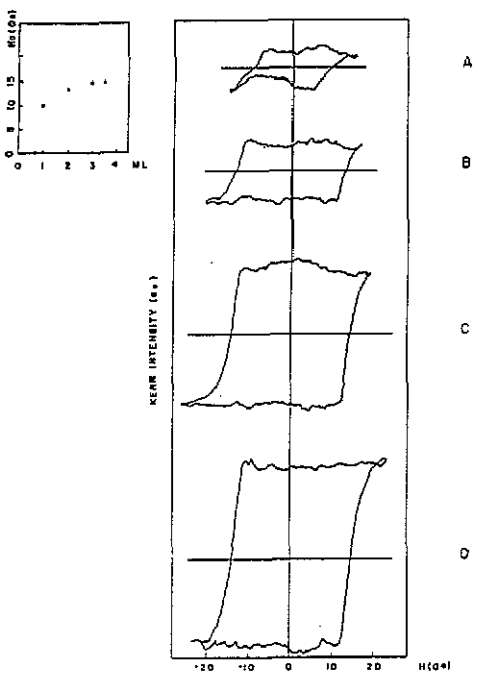

Figure 4. The longitudinal hysteresis loops for one to four layers of Co on Cu(100) thin films. The coercivity ranges from 9.5 Oe for one monolayer of Co on Cu(100) to 14 Oe for four layers of Co on Cu(100) thin films. The vertical scale is the MOKE intensity which is proportional to the Kerr rotation angle. (A), (B), (C), and (D) are for one to four layers, respectively, of Co on Cu(100) thin films.

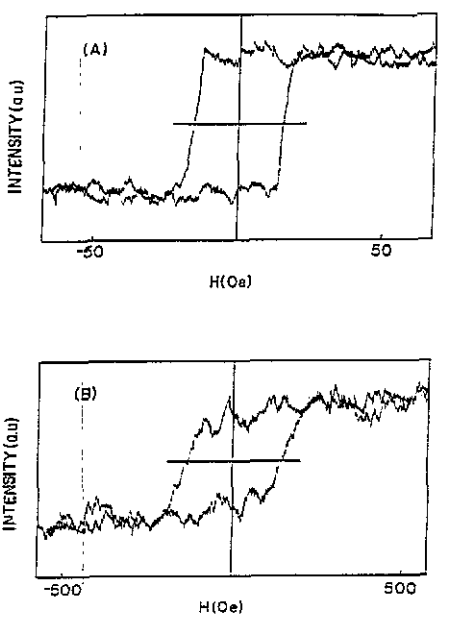

Figure 5. The longitudinal and polar MOKE hysteresis loops for two layers of Co on Cu(100) thin film. (A) and (B) are for longitudinal and polar MOKE hysteresis loops. The coercivity is 14 Oe for longitudinal geometry and 140 Oe for polar geometry. The remanence is 100% for longitudinal geometry and about 100% for remanence for polar geometry.

Figure 5 illustrates the longitudinal and polar MOKE hysteresis loops for two layers of Co on Cu(100). The longitudinal hysteresis loop, as illustrated in figure 5A, exhibits 100% remanence with coercivity of 14 Oe, which is similar to the results obtained by other investigators [14]. The polar hysteresis loop, as illustrated in figure 5B, exhibits reduced squareness with a much higher coercivity of 140 Oe. The surprising bistability

of magnetization along both longitudinal and polar directions will be discussed elsewhere [16]. The presence of a finite slope in the polar hysteresis loop can be attributed to the presence of the demagnetization field, which comes out of Maxwell's equations naturally and can be understood in the GL mean-field theory below.

Figure 6 illustrates the longitudinal hysteresis loops for (four, five) layers of Co/two layers of Cu/four layers of Co trilayers on Cu(100) and (four, five) layers of Co/five layers of Cu/four layers of Co trilayers on Cu(100). As figure 6 illustrates, the magnitude of the hysteresis loops changed dramatically as the thickness of the top Co film increased from four to five atomic layers and the thickness of the Cu interlayer was fixed. Although the magnitude of the Kerr rotation angle changed dramatically, the coercivity remained virtually constant at approximately 40 Oe with excellent squareness, indicating that magnetic easy axes remained the same while the magnetic coupling changed. The data in figure 6 are, however, quite surprising in one respect. The decrease in Kerr rotation angle indicated that the top and the bottom Co layers coupled antiferromagnetically. The antiferromagnetically coupled moments should deviate from antiparallel alignment as the applied magnetic field increased to yield a finite slope in the hysteresis loop. However, we did not observe such a slope in the hysteresis loop.

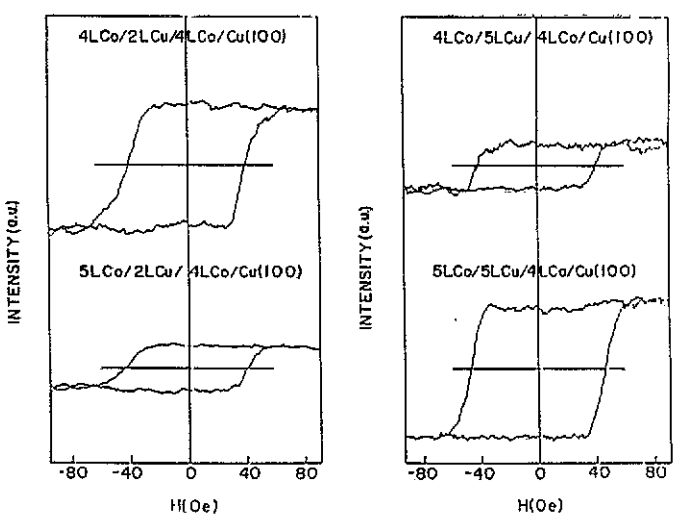

Figure 6. The longitudinal hysteresis loops for (four, five) layers of Co/two layers of Cu/four layers of Co trilayers on Cu(100) and (four, five) layers of Co/five layers of Cu/four layers of Co trilayers on Cu(100). The coercivity are about 40 Oe. The remanence are 100% of the saturation magnetization. The vertical scale is the MOKE intensity for the systems. (A) and (B) are for (four, five) layers of Co/two layers of Cu/four layers of Co trilayers on Cu(100). (C) and (D) are for (four, five) layers of Co/five layers of Cu/four layers of Co trilayers on Cu(100).

Our segregation studies at the Co and Cu interface [12] established that there was no interdiffusion between Co and Cu when the thin-film Co and Co/Cu/Co trilayers were grown on Cu(100) at room temperature. The diffraction studies indicate that these systems exhibit the same excellent diffraction patterns as the layer thickness changed. This indicates that the changes in the measured Kerr rotation angles in

Co/Cu/Co trilayers on Cu(100) were not due to changes in the crystalline structure, but as a manifestation of the changes of the relative orientation of the magnetization of the top and bottom Co layers.

4. Ginzburg–Landau formalism

There have been several reports applying the GL mean-field theory in magnetic systems [9, 10, 17–20]. All of these reports indicate that the GL mean-field theory can provide qualitative agreement with experimental results.

The Gibbs free energy per unit volume in the GL formulation is [10, 17–19]

$$f(r) = f_0(r) + \frac{A}{2}(M(r))^2 + \frac{B}{4}(M(r))^4 + \frac{C}{2}\sum_{i=1}^{3}(\nabla M_i(r))^2 - \tfrac{1}{2}M(r)\cdot H^m - M(r)\cdot H. \tag{2}$$

The first term f_0 is the free energy per unit volume in the absence of magnetization. The order parameter is the magnetization of the film $M(r)$. The fields H^m and H are the demagnetization and applied magnetic fields respectively. The GL coefficients A, B, and C are temperature-dependent parameters. The static magnetization of the system is found for the system with minimum free energy, that is $\partial F/\partial M(r) = 0$. In order for the total free energy F to have a minimum, it is necessary that B and C are always positive. For ferromagnetic and paramagnetic materials, A is positive for $T > T_c$, and for ferromagnetic materials, A is negative for $T < T_c$ [21].

In earlier work [11, 20], we defined the magnetization $M(r)$ as a vector with the following form:

$$M(r) = M_{\parallel}(r)\hat{z}_{\parallel} + M_{\perp}(r)\hat{z}_{\perp} \tag{3}$$

where the z-axis is along the normal of the surface plane and $M_{\parallel}(r)$ and $M_{\perp}(r)$ are components of magnetization parallel and perpendicular to the surface plane. Since the film thickness is very thin compared with the size of the sample surface area, the dependence of magnetization on x and y is much weaker than the dependence on z. We can make the approximation that $M(r) = M(z)$.

For $M_{\perp}(z) = 0$, we obtain

$$-C\,\mathrm{d}^2M_{\parallel}(z)/\mathrm{d}z^2 + AM_{\parallel}(z) + BM_{\parallel}^3(z) = 0 \tag{4}$$

for while $M_{\parallel}(z) = 0$, we obtain

$$-C\,\mathrm{d}^2M_{\perp}(z)/\mathrm{d}z^2 + AM_{\perp}(z) + BM_{\perp}^3(z) = H_{\perp}^m. \tag{5}$$

The demagnetization field H^m is zero when $M_{\perp}(z) = 0$ and non-zero when $M_{\parallel}(z) = 0$. The hysteresis loops for the two magnetizaiton geometries will be different. For $H^m = 0$, the magnetic hysteresis loop may be expected to be quite square if the applied magnetic field direction is along one of the easy axes. For situations where equation (5) applies, the demagnetization field works against the applied magnetic field H, which results in a hysteresis loop deviating from 'square' shape. This agrees with our data and a number of other experimental studies [15, 22]. Magnetic hysteresis loop measurements indicated that the easy magnetization axes were in the film plane. As has been done elsewhere [11, 20], we only need to consider the parallel component of magnetization, $M_{\parallel}(z)$.

As discussed in detail elsewhere [20], solutions to equation (4) exist. Casting in the form of incomplete elliptic integrals $F(\alpha, r)$, standard identities [23] enable the results to be found for $a < -(4|b|)^{-1}$:

$$\beta z = F(\alpha(z), r) - F(\alpha(0), r) \tag{6}$$

where $\beta = 2(ab)^{1/4}\kappa$, and $\alpha(z)$ is defined as follows:

$$\cos\alpha(z) = (m^2(z) - 1)/(m^2(z) + 1) \tag{7}$$

where $m(z) = (b/a)^{1/4}M(z)$ and

$$r = [\tfrac{1}{2} + \tfrac{1}{4}\sqrt{(ab)^{-1}}]^{1/2} \tag{8}$$

and $1/\sqrt{2} \leqslant r \leqslant 1$. The standard expression of $F(\alpha, r)$ is

$$F(\alpha, r) = (2/\pi)K\alpha - \sin\alpha\cos\alpha\ (a_0 + \tfrac{2}{3}a_1\sin^2\alpha + \text{higher-order terms}) \tag{9}$$

where $K = (\pi/2)[1 + (r/2)^2 + \text{higher-order terms}]$ and $a_0 = (r/2)^2$. It has been shown in previous work [20] that the magnetization profile of rare-earth metal overlayers on metal substrate exhibit monotonically varying functional form. We only need the leading term $(2K/2)\alpha$ in rare-earth thin-film systems and the additional terms in equation (9) are small compared with the first term $(2K/\pi)\alpha$. This implied that $a \ll -(4|b|)^{-1}$ [11]. For thin films Co on Cu(100), the experimental magnetization profiles exhibit both a partial monotonic and oscillatory behaviour. In order to obtain agreement with a GL model one can include the higher-order terms, such as a_0 in (9) and note that the condition of $a \ll -(4|b|)^{-1}$ applicable for the rare-earth overlayers [20] no longer holds. As a first-order correction, we take only the a_0-term of (9) into account and all other higher-order terms are neglected. Since a_0 is the higher-order term, we approximate the phase $\alpha(z)$ in the higher-order terms as $\alpha(z) = \alpha(0) + (\pi\beta/2K)z$, which yields the following equation:

$$\beta z = (2/\pi)K(\alpha(z) - \alpha(0)) - a_0\{\sin(2[\pi\beta/2K)z + \alpha(0)] - \sin(2\alpha(0))\}. \tag{10}$$

Redefining $\beta = \pi\beta/K$ and $a_0 = (\pi/2K)a_0$ in equation (10), we obtained the solution for magnetization $m(z)$ in Co film:

$$m(z) = \frac{m(0)}{1 + m(0)\beta z} + \frac{a_0}{2}m^2(0)\left(\sin\frac{4}{m(0)}(1 + m(0)\beta z) - \sin\frac{4}{m(0)}\right). \tag{11}$$

This is, however, clearly an approximation. The magnetic overlayer will exhibit an enhanced magnetic moment per atom due to the reduced dimensionality as the film thickness decreases, and the interface energy (Cu/Co) is neglected.

5. Discussion

Since the penetration depth of the incident photons is much larger than the film thickness, the light was essentially sampling the whole film. The deviation of the functional form of the Kerr rotation angle for thin Co film on Cu(100) from linear or logarithmic form, as illustrated in figure 1, clearly indicates that the large and localized magnetic moment model used for rare-earth overlayers [20] is not valid for Co overlayers on Cu(100) [24]. The self-magnetization energy no longer dominates as it does in the heavy rare-earth metals.

We performed calculations using Dr Samuel Bader's code [25] and established that the effects of the optical constants cannot explain our MOKE Co-thickness-dependent

data. As for the trilayer systems, the additivity rule holds [25]. This indicates that the observed variation of Kerr rotation angle, as illustrated in figure 3, can be attributed as the changes of the relative orientation of the magnetization of the top and the bottom Co layers. The variation of the effective magnetic coupling with the thickness of the top Co layer contradicts the traditional RKKY theory, which does not take into account the effect of interface boundary conditions on the magnetic coupling.

5.1. Hysteresis loop

The magnetic hysteresis loops, as illustrated in figure 4 for thin Co films on Cu(100), exhibit excellent squareness with a very low coercivity of about 14 Oe. The remanence is 100% of the saturation magnetization within experimental error. This is consistent with the results of other investigators [26] that monolayer-range magnetic film possesses a single domain. We postulate that due to the formation of flat surfaces, as confirmed by electron diffraction measurements, there are fewer pinning sites to pin down the domain wall. Such a thin magnetic film also possesses very low magnetic crystalline anisotropy in the plane of the film. As a result, a small driving field can push this 'soft twisted spring' [15] to move forward smoothly when the applied magnetic field is along a magnetic easy axis.

The polar MOKE hysteresis loop, as illustrated in figure 5 for two layers of Co on Cu(100), exhibits a much higher coercivity (140 Oe) than that of the longitudinal hysteresis loop. The remanence was reduced from 100% of the saturation value in the longitudinal geometry to approximately 70% of the saturation magnetization in the polar geometry for two layers of Co. The large increase in coercivity in the polar geometry arises from the effects of the demagnetization field (equation (5)).

As illustrated in figure 6, the coercivity for the Co/Cu/Co trilayers on Cu(100) increased from 14 Oe to about 40 Oe, still very low. The squareness of the hysteresis loop remained almost the same, indicating that domain wall motion was still the magnetization reversal mechanism. No multiple steps were observed in our hysteresis loop measurements. This strongly supports our inference that the domains in the top and the bottom Co films were strongly coupled, and that there cannot be many pinning sites to pin down the domain walls. This strongly indicates that the trilayers we fabricated are well ordered with sharp interfaces.

There is a surprising result in figure 6, which is that the squareness and coercivity of the hysteresis loops for trilayer systems remained almost unchanged when the MOKE signal decreased significantly, indicating the magnetic coupling has changed from ferromagnetic to antiferromagnetic coupling. Our inference is rather bold, namely that the trilayers possessing antiferromagnetic coupling are very strongly coupled and exhibit metamagnetic behaviour. Recall that a distinguishing characteristic of a metamagnetic system is the presence of two (or more) non-parallel magnetic sublattices that are strongly coupled to each other [19, 27]. With such a strong coupling between sublattices, the sublattices respond to a weak applied magnetic field by rotating *as a unit*. Only when the applied magnetic field establishes an energy comparable to the coupling energy between sublattices is the magnetization of the sublattices forced into alignment with the applied magnetic field. We argue that the trilayer systems are exhibiting precisely this type of magnetic behaviour. The hysteresis loops in figure 6 represent the top- and bottom-layer magnetization vectors rotating together *without changing the relative orientation*. However, we have not proven this inference experimentally simply because we are not able to apply such high magnetic fields.

5.2. Thin Co film on Cu(100)

As figure 1 illustrates, there are eight data points for the Kerr rotation angle measurements for one to nine layers of Co on Cu(100). The experimental error bar was 0.03 mrad as determined by the reproducibility of our data from one film deposition to the next. The data clearly indicated that the Kerr rotation angles varied with the thickness of the Co layer that deviated from a logarithmic form. It is rather a mixture of a logarithmic and an oscillatory functional form. The maximum deviation from a logarithmic form occurs at four layers of Co on Cu(100). The oscillatory character of the solution also is seen in GL mean-field theory. This comparison suggests that Co does not possess a large and localized moment and the self-magnetization energy no longer dominates as is the case for rare-earth overlayer films [20]. Equation (11) was easily fitted to the data with four free parameters, as illustrated in figure 1. The fitting parameters used in (11) are $m(0) = 2.1$, $k = 0.07$/layer, $\beta = 0.12$/layer, and $a_0 = 0.45$.

5.3. Co/Cu/Co on Cu(100) trilayers

Figure 2 illustrates the measured Kerr rotation angles for Co/Cu/Co trilayers on Cu(100) with the top- and bottom-Co-layer thicknesses fixed at four atomic layers. The data strongly indicated that the effective magnetic coupling has switched from ferromagnetic to antiferromagnetic as the thickness of the interlayer Cu changed from four to five atomic layers.

Figure 3 illustrates the experimental data for Co/Cu/Co trilayers on Cu(100). The bottom-Co-layer thickness was fixed at four atomic layers. For each thickness of the interlayer Cu, the top-Co-layer thickness was changed from two to five layers for the top panels of figure 3, as discussed before. When the top Co films were one to three layers thick, the top and the bottom Co films were coupled antiferromagnetically. As the top-Co-film thickness reached four atomic layers, the top and bottom layers began to couple ferromagnetically with a significant increase of Kerr rotation angle. As the thickness of the top Co film increased to five atomic layers, the top and bottom Co magnetizations now coupled antiferromagnetically with a dramatic decrease of Kerr rotation angle.

For figure 3, bottom left, the magnetization in the top and bottom Co layers will be forced into parallel alignment by the applied magnetic field and remain in a ferromagnetically coupled state after the applied magnetic field is removed. The Kerr rotation angles will increase monotonically, as illustrated in figure 3, bottom left. For figure 3, bottom right, the interlayer Cu was five layers thick and for one to three layers of Co, the top and bottom Co layers were coupled ferromagnetically with a monotonic increase of Kerr rotation angle. As the thickness of the top Co film increased to four layers, the magnetization between the top Co layer and the Cu layers reversed its direction and the top and bottom Co layers were coupled antiferromagnetically with a significant decrease of Kerr rotation angle. For the top Co film five layers thick, the top and bottom Co layers coupled ferromagnetically with an increase of Kerr rotation angle.

From our experimental data there is a clear indication that the direction of magnetization at the interface between Cu and top Co layer changes as the thickness of the top Co layer changes. We suggest on the basis of these data, that there is a change of direction of the interface magnetization, due to the change of the thickness of the top Co layer. This results in a change of the effective magnetic coupling

between the magnetization of the top and bottom Co layers. Such a postulate would reinforce the importance of the interface magnetization and the complexity of the boundary conditions in determining the effective magnetic coupling in multilayer systems.

6. Conclusion

We have fabricated thin Co films and Co/Cu/Co trilayers on Cu(100) and studied the magnetic properties using magneto-optic Kerr effect spectroscopy. Our data for a thin Co film exhibit neither a linear nor a logarithmic increase in Kerr rotation angle with film thickness. The Kerr rotation angles for trilayer systems oscillate with the thickness of both the interlayer Cu and the top Co layer. The magnetization direction was along the easy axis in the sample plane for all experiments. The squareness of the magnetic hysteresis loop indicated that the magnetization reversal was via domain wall motion with very few pinning sites. This also indicates the high quality of our films with sharp interfaces. No multi-steps in the hysteresis loops were observed in trilayer systems, indicating that the top and the bottom Co films were strongly coupled. The shape of the hysteresis loop remained the same square shape, with coercivity of 40 Oe for trilayers, indicating that the domain walls in the top and the bottom Co films were coupled and moved smoothly together. The lack of slope in the hysteresis loop with antiferromagnetic coupling between the top and the bottom Co layers indicates that the magnetization profiles in the remanence state were energetically stable. The theoretical analysis suggests that the itineracy and relatively small magnetic moment per atom for Co, compared with the heavy rare-earth metals, contributed mainly to the oscillatory behaviour in the magnetization profiles for thin Co films on Cu(100).

Acknowledgments

The authors benefited from conversations with Chian Liu, Samuel Bader, Dongqi Li, Allen Miller, and Robert Joynt. A critical reading of the manuscript by Robert Joynt and Dongqi Li and several discussions are deeply appreciated. The use of the optical response code written by Elizabeth Moog, Samuel Bader and colleagues, is greatly appreciated. We are grateful for the financial support provided by IBM Corporation and the DOE. IBM Corporation, however, does not guarantee or otherwise warrant any of the results contained herein.

References

[1] Falicov L M, Pierce D T, Bader S D, Gronsky R, Hathaway K B, Hopster H J, Lambeth D N, Parkin S S P, Prinz G A, Salamon M, Schuller I K and Victora R H 1990 *J. Mater. Res.* **5** 1299

[2] Esaki L and Tsu R 1970 *IBM J. Res. Dev.* **14** 61

[3] Freeman A J, Xu J and Jarlborg T 1983 *J. Magn. Magn. Mater.* **31–4** 909

[4] Binder K and Landau D P 1984 *Phys. Rev. Lett.* **52** 318 and references therein

[5] Demokritov S, Wolf J A and Grunberg P 1991 *Europhys. Lett.* **15** 881
Parkin S S P, More N and Roche K 1990 *Phys. Rev. Lett.* **64** 2304
Petroff F, Barthelemy A, Mosca D H, Lottis D K, Fert A, Schroeder P A, Pratt W P Jr, Laloee R and Leqvien S 1991 *Phys. Rev.* B **44** 5355
Speriosu V S, Dieny B, Humbert P, Gurney B A and Lefakis H 1991 *Phys. Rev.* B **44** 5358

Parkin S S P, Bhadra R and Roche K P 1991 *Phys. Rev. Lett.* **66** 2152
Mosca D H, Petroff F, Fert A, Schroeder P A, Pratt W P Jr, Laloee R and Lequien S 1991 *J. Magn. Magn. Mater.* **94** 3169
Cochran J F, Rudd J, Muir W B, Heinrich B and Celinski S 1990 *Phys. Rev.* B **42** 508
[6] Pescia D, Kerkmann D, Schumann F and Gudat W 1990 *Z. Phys.* B **78** 475
[7] Majkrzak C F, Cable J W, Kwo J, Hong M, McWhan D B, Yafet Y, Waszczak J V and Vettier C 1984 *Phys. Rev. Lett.* **52** 318 and references therein
Maeda A, Satake T and Kuroda H 1991 *J. Phys.: Condens. Matter* **3** 5241
[8] Heinrich B, Celinski Z, Cochran J F, Muir W B, Rudd J, Zhong Q M, Arrott A S, Myrtle K and Kirschner J 1990 *Phys. Rev. Lett.* **64** 673
[9] Edwards D M, Mathon J, Muniz R B and Phan M S 1991 *Phys. Rev. Lett.* **67** 493
[10] Schwenk D, Fishman F and Schwabl F 1988 *Phys. Rev.* B **38** 11618
Schmidt H and Schwabl F 1978 *Z. Phys.* B **30** 197
Akhiezer A J, Baryakthar V G and Peletminskii S V 1968 *Spin Waves* (Amsterdam: North Holland)
Fishman F, Schwabl F and Schwenk D 1987 *Phys. Lett.* **121A** 192
[11] Miller A and Dowben P A 1992 *Phys. Rev.* B submitted
[12] Chen Qibiao, Onellion M and Wall A 1991 *Thin Solid Films* **196** 103
[13] Gonzalez L, Miranda R, Salmeron M, Verges J A and Yndurain F 1981 *Phys. Rev.* B **24** 3245
Clark A, Jennings G, Willis R F, Raus P J and Pentry J B 1987 *Surf. Sci.* 187 327
Cebollada A, Gellego J M, de Miguel J J, Miranda R, Martinez J L, Ferrer S, Fillion G and Rebonillat J P 1990 *Vacuum* **41** 482
Arnott M, Clark A, Rous P J, Jennings G and Willis R F 1988 *Vacuum* **38** 237
[14] Beier T, Jahrreiss H, Pescia D, Woike T and Gudat W 1988 *Phys. Rev. Lett.* **61** 1875
Schneider C M, Bressler P, Schuster P, Kirschner J, de Miguel J J, Miranda R and Ferrer S 1990 *Vacuum* **41** 503
Bland J A C, Padgett M J, MacKayand K D and Johnson A D 1989 *J. Phys.: Condens. Matter* **1** 4407
Lee C H, He Hui, Lamelas F J, Vavra W, Uher C and Clark Roy 1990 *Phys. Rev.* B **42** 1066
Pescia D, Zampieri G, Stampanoni M, Bona G L, Willis R F and Meier F 1987 *Phys. Rev. Lett.* **58** 933
Bland J A C, Pescia D and Willis R F 1987 *Phys. Rev. Lett.* **58** 1244
[15] Cullity B D 1972 *Introduction to Magnetic Materials* (New York: Addison-Wesley)
[16] Chen Qibiao, Onellion M and Wall A 1992 *J. Magn. Mater.* submitted
[17] Landau L and Lifshitz E M 1984 *Electrodynamics of Continuous Media* 2nd edn (revised and enlarged) (Oxford: Pergamon)
[18] LaGraffe D, Dowben P A, Miller A and Onellion M 1991 *Mater. Res. Soc. Symp. Proc.* **187**
[19] Mills D L 1971 *Phys. Rev.* B **3** 1887
Suhl H 1975 *Appl. Phys.* **8** 217
[20] Dowben P A, LaGraffe D, Li Dongqi, Miller A, Zhang L, Dottl L and Onellion M 1991 *Phys. Rev.* B **43** 3171
[21] Kadanoff L P, Gotze W, Hamblem D, Hecht R, Lewis E A S, Palciauskas V V, Rayl M, Swift J, Aspnes D and Kane J 1967 *Rev. Mod. Phys.* **39** 195
[22] Liu C, Moog E R and Bader S D 1988 *Phys. Rev. Lett.* **60** 2422
[23] Gradshteyn I S and Ryzhik I M 1980 *Tables of Integrals, Series, and Products* (corrected and enlarged edition) (New York: Academic) p 260, formula 3.165, #2
[24] For materials possessing a large and localized moment, the self-magnetization energy dominates. As a result, the magnetization profile derived from mean-field theory exhibits monotonically varying behaviour. See [20] for more detail.
[25] Zak J, Moog E R, Liu C and Bader S D 1990 *J. Appl. Phys.* 68 4203
[26] Robins J L, Celotta R J, Unguris J, Pierce D T, Jonker B T and Prinz G A 1988 *Appl. Phys. Lett.* **52** 1918
Scheinfein M R, Unguris J, Blue J L, Coakley K J, Pierce D T and Celotta R J 1991 *Phys. Rev.* B **43** 3395
Farle M, Berghaus A and Baberschke K 1989 *Phys. Rev.* B **39** 4838
[27] Kaneyoshi T 1991 *Introduction to Surface Magnetism* (Boca Raton, FL: Chemical Rubber Company)